2023 IEEE International Conference on Robotics and Automation (ICRA 2023)
May 29 - June 2, 2023. London, UK

Twisting Spine or Rigid Torso: Exploring Quadrupedal Morphology via Trajectory Optimization

J. Diego Caporale[⋆◇], Zeyuan Feng[†◇], Shane Rozen-Levy[⋆], Aja Mia Carter[†], Daniel E. Koditschek[†]

***Abstract*— Modern legged robot morphologies assign most of their actuated degrees of freedom (DoF's) to the limbs and designs continue to converge to twelve DoF quadrupeds with three actuators per leg and a rigid torso often modeled as a Single Rigid Body (SRB). This is in contrast to the animal kingdom, which provides tantalizing hints that core actuation of a jointed torso confers substantial benefit for efficient agility. Unfortunately, the limited specific power of available actuators continues to hamper roboticists' efforts to capitalize on this bio-inspiration. This paper presents the initial steps in a comparative study of the costs and benefits associated with a traditionally neglected torso degree of freedom: a twisting spine. We use trajectory optimization to explore how a one-DoF, axially twisting spine might help or hinder a set of axially-active (twisting) behaviors: trots, sudden turns while bounding, and parkour-style wall jumps. By optimizing for minimum electrical energy or average power, intuitive cost functions for robots, we avoid hand-tuning the behaviors and explore the activation of the spine. Initial evidence suggests that for lower energy behaviors the spine increases the electrical energy required when compared to the rigid torso, but for higher energy runs the spine trends toward having no effect or reducing the electrical work. These results support future, more bio-inspired versions of the spine with inherent stiffness or dampening built into their mechanical design.**

I. Introduction

A. Motivation

State of the art and commercially available [1] [2] [3] quadrupedal robot morphology has converged around the twelve degree-of-freedom (DoF), 3DoF legged, rigid torso robots similar to the MIT Mini-Cheetah [4] or ANYmal [5]. Three DoF legs provide a good compromise of capability, weight, and power density allowing robots to produce 3DoF forces at their toes in most configurations. Adding actuators to the leg design is inherently expensive (both in weight and money) with each addition being made multiple times due to bilateral or quadrilateral symmetry constraints. Turning to biology for inspiration, one can instead explore how different spinal DoFs (replacing the rigid torso) could augment the legs' capabilities and allow new locomotion strategies while reducing overall costs.

The diversity of function that arises from variation in bone geometry and muscle size and attachment within biological spinal columns can be mapped to differences in bending and rotational ability [6]. A great volume of biological and bio-inspired robotics literature has described the roles and functional trade-offs of lateral and sagittal spinal bending during transitions from aquatic to aerial environments, climbing, and dynamical gaits [7]–[16]. In stark contrast, however, is a dearth of literature isolating axial twisting in the spine (i.e., twisting without bending) and investigating the functional role of twisting during any locomotion. Within the biological literature, the role of axial twisting is described only as a stabilizing measure against long-axis rotation generated by ground reaction forces while moving through periodic locomotor behaviors [8] [14] [16]. Insights gained from bio-inspired robotic design and exploration can be used as a model (physical and numerical) to generate new functional hypotheses in biology for twisting during non-periodic, transitional behaviors.

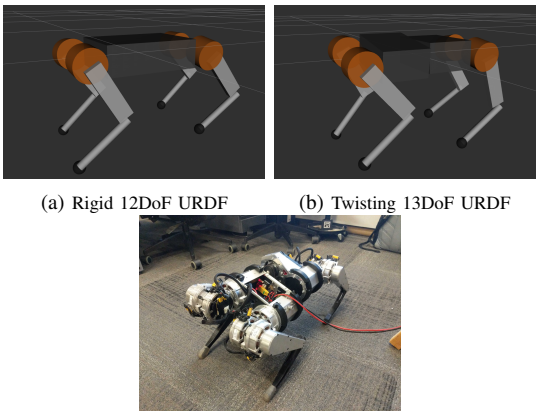

(a) Rigid 12DoF URDF (b) Twisting 13DoF URDF

(c) Twist, 13DoF Quadruped

Fig. 1: Quadrupedal Models and Real World System: (a, b) Visualizations of the two URDF's used in the optimization. They are identical except for a joint in the center of the body. (c) Twist is a prototype, twisting quadruped developed in the Kod*Lab at the University of Pennsylvania by Ethan Musser and J. Diego Caporale.

Bio-inspired robotic designs distill the sufficient features for particular tasks from biological creatures without mimicking their "designs". Beyond the dynamical and control incentives for simplifying morphology, another limiting factor for the inclusion of any specific resource is the actuation and power density available to a robot designer, especially when attempting high power/agile, transitional maneuvers. In light of these mass-specific power constraints, a simple, one degree-of-freedom (DoF) twisting "spine" represents a minimum design enabling the exploration of costs and benefits for various behaviors arising from the added endowment of an axially twisting spine. Before committing to the material pro-

[†] Electrical and Systems Engineering, University of Pennsylvania, PA, USA. {zeyuanf,caja,kod}@seas.upenn.edu
[⋆] Mechanical Engineering and Applied Mechanics, University of Pennsylvania, PA, USA. {jdcap,srozen01}@seas.upenn.edu
[◇] Co-first authors

This work was supported in part by the Vannevar Bush Faculty Fellowship (JDC, ZF) and by University of Pennsylvania Vice Provost of Diversity Fellowship (AMC)

duction of such a design, it is prudent to analyze and model the system. This paper numerically explores the costs and benefits for a variety of spatial maneuvers of a twist-enriched quadrupedal torso by contrasting its potentially achievable optimal trajectories with those of a rigid alternative.

B. Literature review

Abundant evidence demonstrates that spinal degrees of freedom confer energetic, workspace, and stabilizing benefits [17], [18] for legged locomotion in biological creatures. Notwithstanding the likely benefits arising from various structural details (e.g. discrete vertebrae, graded tendon-bone attachment, or skin) of animal spines, their abstraction in bio-inspired robotics (strongly incentivized by the limitations of available synthetic materials and actuation as remarked above), typically yields machine torsos with one or two bulk degrees of freedom. Several quadrupedal robots have incorporated low DoF spines in their design and validated the benefits of spines experimentally [19]–[27] and in simulation [28]–[33] showing that (especially sagittal) spinal DoF's are able to lower power consumption, increase maximum forward speeds and hopping heights, aid in leg recirculation, and stabilize running gaits. In all this exploration, trajectory optimization has been a great low-cost tool for roboticists before committing to simulation and/or hardware.

In quadrupeds, optimization studies have explored the costs and benefits of varied limb morphologies [34], spine morphologies [32], [35]–[37], and spine actuation strategies [25] [38]. Together, they suggest beneficial spinal and limb configurations for periodic running and leaping, for accelerating, and for transitional behaviors. However, all of these studies were confined to the sagittal plane or activating systems purely in the sagittal plane, significantly reducing their complexity. Analyzing axial twisting in the sagittal plane is not possible for most behaviors without making overly simplifying or constraining assumptions. Beyond that, the maneuvers highlighted in this work are not describable without a spatial, 3D description of the robot and dynamics.

The increase in complexity in the optimization makes it more difficult to get consistent and accurate results from the nonlinear program solvers. Thus, optimization methods can be fraught with design choices as well, and care must be taken in choosing cost functions [39], constraints, and tuning parameters as well as comparative metrics and experiments.

C. Contributions and Organization

In this paper, we use trajectory optimization with a detailed, fully spatial model to explore how a previously neglected torso degree of freedom —the twisting spine — might help or hinder quadrupedal robot, Fig. 1.
In order to gain insight of the effect of a twisting spine,

- Sections II develops a DIRCON-based [40] trajectory optimization pipeline in Drake [41] capable of testing and comparing a variety of different behaviors on quadrupeds in full 3D space.
- Section III lays out a representative set of behaviors and corresponding metrics to compare between morphologies.
- Section IV explores the benefits and disadvantages of a twisting spine relative to a conventional torso in the trot, bounding turn, and wall leap behaviors.
- Section V discusses possible ramifications for robotic design and biological hypotheses.

II. Methodology

A. Trajectory Optimization

Trajectory optimization is a class of optimal controls techniques for finding the best set of control inputs and states subject to a set of constraints and a cost function [42]. Generally, trajectory optimization problems are solved by converting the infinite dimensional optimization over functions into an approximately equivalent finite dimensional optimization over scalars using direct collocation [43]. The resulting problems can then be solved using standard nonlinear programming (NLP) techniques.

In this paper, we used DAIR Lab's implementation of trapezoidal DIRCON [40] [44]. DIRCON is an extension of direct collocation for constrained dynamical systems which restricts solutions to a constraint manifold without over constraining the optimization problem. This formulation is useful when studying hybrid system like walking robots where each contact with the world can be described as a constraint manifold.

However, one limitation of DIRCON when compared to other state-of-the-art methods like contact-implicit trajectory optimization [45] is that DIRCON requires a known mode sequence. In light of this limitation, we still chose to use DIRCON over contact-implicit methods because the mode sequences for our target behaviors are known a priori and DIRCON can vary each mode's duration, by treating time as decision variables, yielding sufficient richness for contact decisions. However, as a result, the timing of each optimization can require tuning in certain behaviors to avoid having the timestep moved to extremes.

Our target behaviors' mode sequences will be divided into stance and flight phases, for example

$$\mathcal{M}_A = \{\mathcal{S}_{i,j}, \mathcal{F}\}$$

would be the sequence for a behavior, A, that had a stance phase $\mathcal{S}_{i,j}$ with toes i and j in contact and a flight phase $\mathcal{F}$ where no toes are in contact with the ground. The flight is also often separated into two phases — pre and post apex — which we will note as $\mathcal{F}^-$ and $\mathcal{F}^+$ respectively.

B. Dynamic Models

The quadruped is modelled as a floating-base robot composed of rigid links as legs and electrical motors [46].

$$\begin{cases} \mathbf{M}(\mathbf{q})\ddot{\mathbf{q}} + \mathbf{C}(\mathbf{q},\dot{\mathbf{q}})\dot{\mathbf{q}} + \mathbf{G}(\mathbf{q}) = \mathbf{B}^T\boldsymbol{u} + \mathbf{J}^T\mathbf{F} \\ \mathbf{M}(\mathbf{q})\dot{\mathbf{q}}^+ - \mathbf{M}(\mathbf{q})\dot{\mathbf{q}}^- = \mathbf{J}^T\boldsymbol{\Lambda} \end{cases} \tag{1}$$

where $\mathbf{M}(\mathbf{q})$ is the inertia matrix, $\mathbf{C}(\mathbf{q},\dot{\mathbf{q}})$ is the Coriolis term, $\mathbf{G}(\mathbf{q})$ is the gravitational force. $\boldsymbol{u}$ are motor torques,

Parameter	Value	Parameter	Value
Robot mass	11.45 kg	Hip gear ratio	6:1
Body length	0.335 m	Knee gear ratio	9:1
Body width	0.24 m	Abduction gear ratio	6:1
Upper leg length	0.20 m	Spine gear ratio	6:1
Lower leg length	0.20 m	Ungeared motor	U8 [47]

TABLE I: Model parameters for the rigid and twisting robots

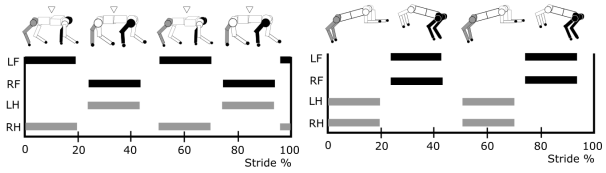

(a) Trot (b) Bound

Fig. 2: Hildebrand Style [49] gait diagram for an idealized trot and bound in Twist. The initials L, R, F, H stand for left, right, fore and hind limbs. Black bars represent forelimb (left or right) is in contact with the ground.

$\mathbf{F}$ are ground contact forces with corresponding jacobians $\mathbf{B}$ and $\mathbf{J}$. $\mathbf{q} = \begin{bmatrix}\mathbf{q}^{bT} & \mathbf{q}^{pT} & \mathbf{q}^{jT}\end{bmatrix}^T$ where $\mathbf{q}^b \in SO(3)$ is the unit quaternion of the base, $\mathbf{q}^p$ is base position in world frame, and $\mathbf{q}^j$ are joint positions. The second row of the equation is the impact dynamics , where $\dot{\mathbf{q}}^+$ and $\dot{\mathbf{q}}^-$ are pre-impact and post-impact joint velocities, and $\mathbf{\Lambda}$ is the impulse.

The rigid robot's parameters are modeled after common 12 motor quadrupeds such as the MIT Mini cheetah [4] or Unitree A1 [3] (Table I). The twisting robot model is based on the rigid robot model with an added twisting spinal joint in the middle of the original base. The rear segment of the trunk serves as the new base. Extra mass and inertia of spinal joint are not considered in this paper.

C. Cost Functions

Cost function choice is important and a poor choice can cause a behavior's optimization problem to fail to converge or converge to unrealistic solutions. Additionally, the goal is to avoid shaping or tuning the behavior with costs (and their gains) and instead to enforce constraints based on each task for a parametric investigations of the problem spaces. A natural cost function for robotic systems is positive electrical energy [39] defined for the jth joint as

$$\theta_j^E(\dot{\mathbf{q}}, \mathbf{u}) = K_{energy} \int_0^{t_f} \max(Q_j \mathbf{u}_j^2 + \dot{\mathbf{q}}_j \mathbf{u}_j, 0) \mathrm{d}t \quad (2)$$

Where $Q_j = \frac{R}{K_t^2 N_j^2}$ maps torque to electrical power, R is the winding resistance, K_t is the torque constant, and N_j is the gear ratio. For periodic behaviors, the goal should be to maintain the cycle with minimum energy over time and so average power is used[1].

$$\theta_j^P(\dot{\mathbf{q}}, \mathbf{u}) = K_{power} \int_0^{t_f} \frac{\max(Q_j \mathbf{u}_j^2 + \dot{\mathbf{q}}_j \mathbf{u}_j, 0)}{t_f} \mathrm{d}t \quad (3)$$

For initializing optimizations and warm-starting, we used quadratic costs on actuation and velocity. The velocity cost is also used to regularize the limbs during flight phases.

$$\theta_j^U(\dot{\mathbf{q}}, \mathbf{u}) = K_{act} \int_0^{t_f} \mathbf{u}_j^2 \mathrm{d}t, \quad \theta_j^V(\dot{\mathbf{q}}, \mathbf{u}) = K_{vel} \int_0^{t_f} (\dot{\mathbf{q}}_j)^2 \mathrm{d}t \quad (4)$$

D. Optimization Formulation

The general optimization setup[2] is given in Equation (5). In addition to the constraints listed in this section, we also include additional behavior specific constraints described in Sec. III-A, Sec. III-B, and Sec. III-C.

$$\begin{aligned}
&\underset{\mathbf{x},\mathbf{u},\boldsymbol{F},t_f}{\text{minimize}} && \sum_{j \in \mathcal{J}} \left(\theta_j^E + \theta_j^P + \theta_j^V\right) && \text{(5a)}\\
&\text{subject to} \\
&\text{(Dynamics)} && \dot{\mathbf{x}} = f(\mathbf{x}, \mathbf{u}, \boldsymbol{F}) && \text{(5b)}\\
&\text{(Impact)} && \mathbf{M}(\mathbf{q}_k)\dot{\mathbf{q}}_k - \mathbf{M}(\mathbf{q}_{k+1})\dot{\mathbf{q}}_{k+1} = \mathbf{J}_k^T \mathbf{\Lambda}_i && \text{(5c)}\\
&\text{(Friction)} && \sqrt{\mathbf{F}_x^2 + \mathbf{F}_y^2} \leq \mu \mathbf{F}_z && \text{(5d)}\\
&\text{(Acceleration)} && |\ddot{\mathbf{q}}| \leq \ddot{\mathbf{q}}_{max} && \text{(5e)}\\
&\text{(Duration)} && t_{min} \leq t_f \leq t_{max} && \text{(5f)}\\
&\text{(Torque limits)} && u \leq U(\dot{q}) && \text{(5g)}\\
&\text{(Toes height)} && \bar{f}_t(\mathbf{x}) \geq 0 && \text{(5h)}\\
&\text{(Joint limit)} && \mathbf{q} \in \mathcal{Q} && \text{(5i)}
\end{aligned}$$

where U is a linear speed torque curve based on parameters from [47] for the T-Motor U8 and $\bar{f}_t(\cdot)$ is the forward kinematics that returns the t^{th} toe's height. The spinal joint is treated like any other joint with its limits subsumed into the above description and other constraints are kept fixed wherever possible to properly isolate the added DoF.

E. Summary of Optimization Procedure

We use an automated optimization pipeline to generate various, locally optimal trajectories throughout the parameter space of the behaviors. The optimization process[2] starts with a rough, initial guess and finds solutions across the parameter space (e.g. low speed to high speed or short jump to long jump) using rigid constraints and quadratic costs. For each parameter sampling, the pipeline then progressively relaxes the constraints and changes to more natural cost functions (Section II-C). Simultaneously, the pipeline runs each sample many times with different random noise thereby exploring the landscape around the local minima. All the trajectories shown are produced with the final optimization setups, with the costs and constraints described in each respective section (Sec. II-D, Sec. III-A, Sec. III-B, and Sec. III-C)

III. Behaviors

We tested our pipeline on three different behaviors: a trot III-A, a yawing bound III-B, and a parkour wall jump III-C.

[1]Using total energy in a periodic behavior incentivizes the optimization to shorten the period resulting in tiny steps.

[2]For more detail about the optimization setup and pipeline, refer to the detailed README in the git repository [48]

A. Trot

In addition to our primary hypothesis — a twisting spine is beneficial in high-power transitional behaviors — we also investigated a basic functional gait (i.e., trotting) for a quadruped. The trot is the preferred gait for many quadrupedal robots and it is not symmetric across the sagittal plane. The trot is characterized by diagonal contact pairs without a four-legged stance (Fig. 2a). The mode sequence is

$$\mathcal{M}_{trot} = \{\mathcal{F}^+, \mathcal{S}_{\text{LF,RH}}, \mathcal{F}^-, \mathcal{F}^+, \mathcal{S}_{\text{RF,LH}}, \mathcal{F}^-\}.$$

However, to simplify the optimization the trot is optimized as a half-period with a mirror reset map. Therefore, the trot mode sequence is

$$\mathcal{M}_{halftrot} = \{\mathcal{F}^+, \mathcal{S}_{\text{LF,RH}}, \mathcal{F}^-\}$$

and the reset map is a mirroring of the state and input across the sagittal plane. Note that the trot can have a trivial four legged stance phase (by making the flight phase close to zero time), but cannot truly walk or stand.

The optimization problem for the trot is given by Equation (5) with gains $K_{power} = 100$ for all modes and $K_{vel} = 1$ in flight (all other costs are zero). Additionally, the trot is setup using the following constraints. The average velocity is constrained to $\frac{\mathbf{x}_{x,f} - \mathbf{x}_{x,0}}{T} = v_{target}$ and the robot is constrained to the plane with $\dot{\mathbf{x}}_y = \mathbf{0}$, where $\mathbf{x}_{x,f}$ is the final x-position, $\mathbf{x}_{x,0}$ is the initial x-position, T is time span of the period, and $\dot{\mathbf{x}}_y$ is the velocities along y axis at all times along the trajectory. The legs that are in contact have an additional constraint on leg length to prevent the optimizer from abusing the singularity at low speeds. Finally, the trot's periodicity is enforced at the initial and final states by a mirrored reset constraint.

B. Bounding Turn

In contrast to the trot, a bound is a behavior where we expect low twisting spine activation due to bilaterally symmetrical contacts. The bound is characterized by alternating fore and aft toe contact pairs as seen in Fig. 2b with the mode sequence

$$\mathcal{M}_{bound} = \{\mathcal{F}^+, \mathcal{S}_{\text{LF,RF}}, \mathcal{F}^-, \mathcal{F}^+, \mathcal{S}_{\text{LH,RH}}, \mathcal{F}^-\}.$$

The bounding contact pattern gives the opportunity to isolate the twisting spine activation from the gait itself and thus we explore a quick-turn transitional behavior. In the bounding turn, the robot is asked to make a sudden turn — changing yaw and velocity heading — over the course of a single stride without disturbing the previous or following bounds. Although this behavior itself is not practical or biologically realistic, exploring it still gives a qualitative look at how a spine might help absorb the impulses from turning. We hypothesize any activation of the spine is caused by the turn and the impulses required to do so.

The optimized cost in the steady state bound is, as with the trot, average power (Eq. 3) and a regularizing cost on leg velocity during flight (Eq. 4). Meanwhile, the yawing, single-stride turn optimizes the positive electrical energy consumption (Eq. 2) for transitioning from one steady-state bound to another with the desired new direction. The initial state of yawing turn is constrained to be the final state of a sagittal bound, whereas the final state is constrained to be the initial state of the sagittal bound (which is identical to its final state) rotated by a desired yaw rotation. The roll and pitch angles are limited and reference yaw bounds are imposed on several intermediate states, such as lift-off and touch-down states, to improves the convergence of the optimization problems, however they are inactive in the final optimizations.

C. Wall Jump

The wall jump is a high energy transitional maneuver borrowed from parkour and the animal kingdom. It involves the robot jumping a long distance by taking advantage of a vertical wall. The mode sequence is

$$\mathcal{M}_{walljump} = \{\mathcal{S}_{\text{LF,LH,RF,RH}}, \mathcal{S}_{\text{LH,RH}}, \mathcal{F}^-, \mathcal{F}^+, \mathcal{S}_{\text{LF,RF}}, \mathcal{S}_{\text{LF,LH,RF,RH}}, \mathcal{S}_{\text{LH,RH}}, \mathcal{F}^-, \mathcal{F}^+, \mathcal{S}_{\text{LF,RF}}, \mathcal{S}_{\text{LF,LH,RF,RH}}]\}.$$

The wall jump is characterized by a displacement in the x direction and consists of a leap to and then off the wall. As a fully 3D, transitional maneuver with an inherent axial roll motion, it can potentially help to explore how a quadrupedal robot will take advantage of a twisting spinal joint in complex spatial behaviors.

The cost gains for wall jump are $K_{energy} = 100$ for all modes and $K_{vel} = 5$ in flight. Due to the complexity of the problem, the optimization required careful constraints to prevent infeasible solutions. Both the initial and final state are set to a nominal stance. The initial and final y position, apex heights, and x and z positions of the bottom state on the wall are bounded but not fixed. Where as in the trot and bound we enforce apex between the flight phases, v_z at these knot points are not fixed at zero but rather loosely constrained allowing the optimizer to produce leaps to or from the wall without apexes. We also set loose upper bounds for hip angles and front leg velocities during the flight phases to stabilize the optimization. Most importantly, we enforce some reference orientation bounds for several key knot points, including lift-off states, touch-down states, apex states, and the bottom state on the wall, to shape the feasible region.

IV. Results

We ran a total of 1462, 1500, and 753 optimizations for trot, bounding turn, and wall jump, respectively[3]. The convergence rates of final optimizations for trot, bounding turn and wall jump are 42.91%, 35.67%, and 48.46%. Optimization results are presented in the following sections.

A. Trot

We optimized trot trajectories with target speeds ranging from 0 to 4 m/s and with stride periods ranging from 0.2 to 0.8 s. At lower speeds, the spined robot uses significantly

[3]These numbers include optimizations to find warm starts.

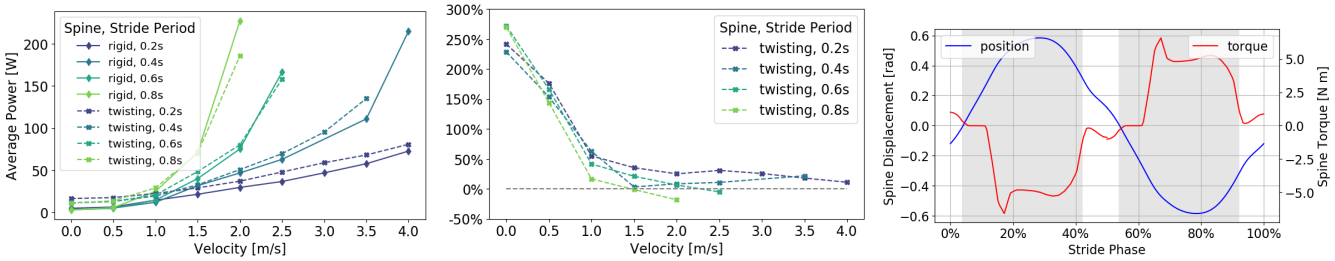

(a) Average power magnitude for trotting in rigid and twisting spine model

(b) Percentage difference in average power of given trots of twisting robot relative to rigid model (gray dashed)

(c) Nominal spinal activation example for 2 m/s trot with a 0.6s period

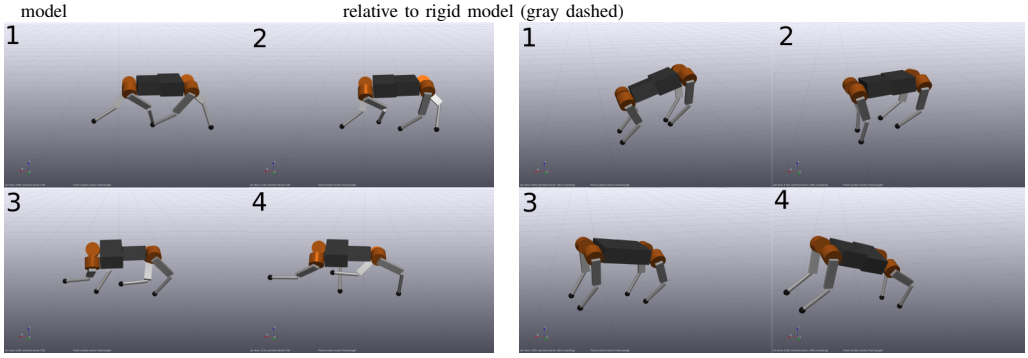

(d) Frames from the trot solution for the twisting spine model with a speed of 2 m/s and a period of 0.6 s

(e) Frames from the turning bound for the twisting spine model with a speed of 2 m/s, a period of 0.3 s, and a yaw of 0.4 rad.

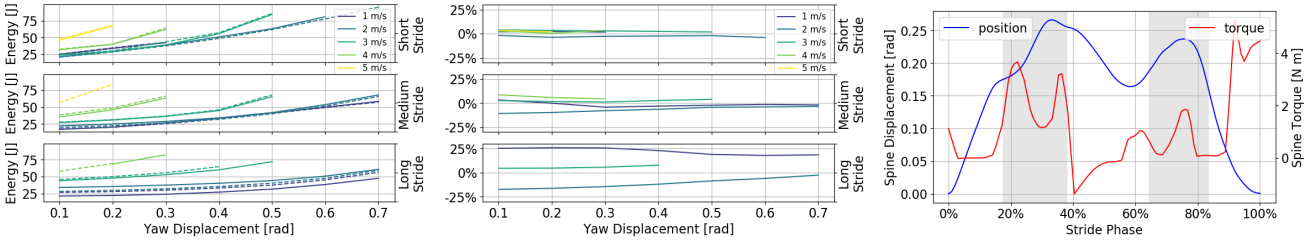

(f) Energy for turning bound. Solid lines are for the rigid model, and dashed are for the twisting model

(g) Percentage difference in energy for several turning bounds of the twisting model relative to the rigid model

(h) Nominal spinal activation example for 2 m/s bound with period of 0.3 s and a yaw of 0.4 rad.

Fig. 3: Quantitative results from the trot and turning bound. (a) shows the magnitude of the average power for rigid and twisting spines for a variety of trots with different stride periods. (b) shows the percentage difference of twisting to rigid average power from (a). As expected the twisting spine requires more energy in the trots, especially at lower speeds. (c) is a nominal spine pose and torque for a trot with a velocity of 2 m/s and a stride period of 0.6 s. (d) is a set of frames taken from the same run shown in (c) showing the activation of a twisting spine in the trot. Likewise, (e) is a set of frames taken a 2 m/s bound with a period of 0.3 s and a yaw of 0.4 rad with spinal activation. (f) shows the magnitude of the average power for rigid and twisting spines for a variety of turning bounds with different stride periods, velocities, and yaw angles. (g) shows the percentage difference of twisting to rigid average power from (f). The twisting spine is beneficial around the 2 m/s velocity bound for twisting robot and is most coupled with the longest stride period (0.4 s), likely due to the pitching. (h) is nominal spine pose and torque for the bound from (e).

more power, likely due to the behavior being quasi-static, forcing the spine to apply torque just to stay still (Fig. 3a, 3b). As the trot gait becomes increasingly dynamic, the difference between the rigid and spined robot becomes less severe. This suggests the trot may benefit from a passive spring system in parallel with the spine to share the base load at lower speeds but which can still be energized at higher speeds.

Figure 3c and 3d demonstrate that even at a modest speed of 2 m/s, there is substantial activation in the spine.

B. Bounding Turn

For the bounding turn, we measured the energy consumption for yawing an angle ranging from 0.1 to 1 radians (or to failure) at a speed ranging from 1 m/s to 5 m/s. For each speed, three steady state bound trajectories with short, medium and long stride lengths (with a period of 0.2 s, 0.3 s, 0.4 s) are used to warm start the NLP and constrain the initial and final states of the yawing turn as described in Sec. III-B. In Figure 3f, we see the power to turn is similar across morphologies. However, in longer strides the twisting spine has mixed effect on energy. At 1 m/s the system requires more energy to turn with the spine, but at 2.0 m/s the energy required relative to the rigid robot is less. The regularity of each of these velocities' data suggests this is not an aberration, but rather some more systematic pattern, suggested by the optimization emerging as a "sweet-spot" for the value of the twisting spine, revealed in the context of fast maneuvers at tight quarters.

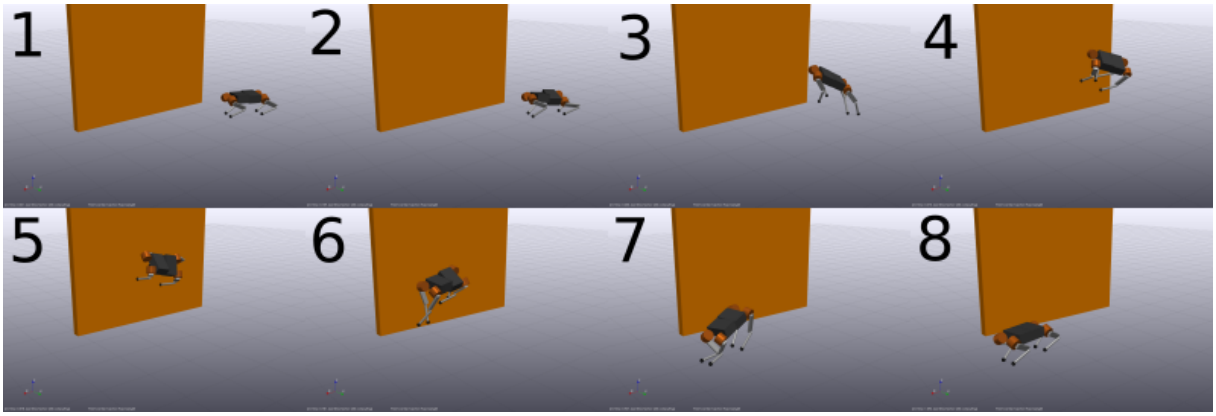

Fig. 4: Renders of the twisting robot completing the 2 m wall jump

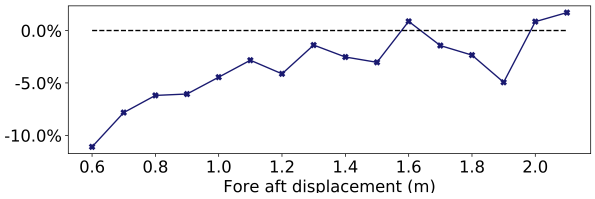

(a) Percentage difference in optimal energy of twisting spine (solid) relative to rigid spine (dashed).

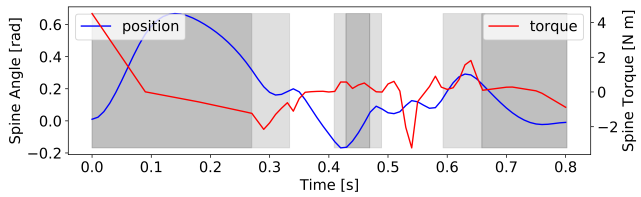

(b) Spine activation for 0.6 m wall jump

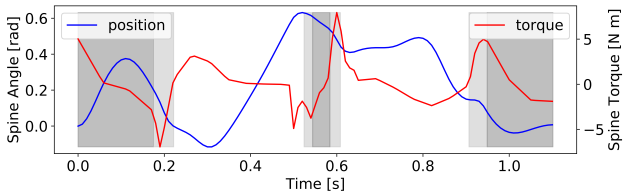

(c) Spine activation for 2.0 m wall jump

Fig. 5: The first figure shows the optimal work difference for twisting spine. Next two figures are spine activation for a 0.6 m jump and a 2.0 m jump, respectively. Dark gray shaded regions specify four-leg stance phases; the light gray regions are in two-leg stance phases; the remaining segments are in flight phases.

C. Wall Jump

For the wall jump, we optimized jumps ranging from 0.5 to 2 m. Figure 4 shows the spined robot completing a 2.0 m wall jump. Figure 5 shows that for the lower distances the spined robot uses significantly less energy than the rigid robot. As the distance increases the robots start to perform similarly. This suggests once again, corroborating evidence for the intuition, that a twisting spine may be particularly beneficial in the specific context of a rapid body reorientation in tight quarters, such as the aggressively rolled legs.

Since the wall jump is a high power behavior with a lot of roll, it matches our hypothesis that the spine is either neutral or beneficial. In the cases where the robot is jumping only a short distance, it seems challenging for the rigid robot to get its front legs onto the wall. As a result the twisting spine robot shines in those behaviors. As the fore-aft distance increases the robots have more time and distance to roll resulting in similar performances between the two robots.

As shown in Figure 5b and 5c, the spine behaves differently under short- and long-distance jumps by orienting the upper body toward and away from the wall respectively. This shows two activation patterns, one which takes advantage of the extra kinematic flexibility in a crowded environment or another which uses a dynamically stronger configuration on the transitional surface to gain more momentum.

V. Discussion and Future Work

In this study, we used DIRCON trajectory optimization to investigate the effect of an internal degree of freedom in a quadrupedal robot. For low energy sagittal plane behaviors like a slow trot, the spine increased the energy usage. The added flexibility requires actuation during the two-legged stance phase to stop from folding in on itself. But, as seen in the results for the high speed trot, bounding turn, wall jump, the spine can be used to absorb some of that stress and at least lessen the impulses to out of plane (non-sagittal) DoF's resulting in similar energy usage between the twisting robot and the rigid robot. These results suggest, as expected, that the twisting spine does not benefit every behavior, though there were sufficient cases where it was helpful, thus requiring further study.

This study marks a necessary first step for internal degrees of freedom outside of bending in quadrupeds. In the future we would like to explore more behaviors, add passive mechanical elements (e.g. springs, dampers, etc.) in parallel with the spine, explore a higher number of spine DoF's, and test some of these optimized behaviors on a real robot (Figure 1c). These results will hopefully lead to the creation of robots whose agility begins to approach that of animals.

REFERENCES

[1] "Boston dynamics spot." [Online]. Available: https://www.bostondynamics.com/products/spot 1

[2] "Ghost robotics." [Online]. Available: https://www.ghostrobotics.io/ 1

[3] "Unitree." [Online]. Available: https://m.unitree.com/ 1, 3

[4] B. Katz, J. Di Carlo, and S. Kim, "Mini cheetah: A platform for pushing the limits of dynamic quadruped control," in *2019 international conference on robotics and automation (ICRA)*. IEEE, 2019, pp. 6295–6301. 1, 3

[5] M. Hutter, C. Gehring, D. Jud, A. Lauber, C. D. Bellicoso, V. Tsounis, J. Hwangbo, K. Bodie, P. Fankhauser, M. Bloesch, R. Diethelm, S. Bachmann, A. Melzer, and M. Hoepflinger, "Anymal - a highly mobile and dynamic quadrupedal robot," in *2016 IEEE/RSJ International Conference on Intelligent Robots and Systems (IROS)*, 2016, pp. 38–44. 1

[6] N. Schilling, "Evolution of the axial system in craniates: morphology and function of the perivertebral musculature," *Frontiers in Zoology*, vol. 8, no. 1, p. 4, 2011. [Online]. Available: http://frontiersinzoology.biomedcentral.com/articles/10.1186/1742-9994-8-4 1

[7] W. Wang, A. Ji, P. Manoonpong, H. Shen, J. Hu, Z. Dai, and Z. Yu, "Lateral undulation of the flexible spine of sprawling posture vertebrates," *Journal of Comparative Physiology A*, vol. 204, no. 8, pp. 707–719, Aug. 2018. [Online]. Available: http://link.springer.com/10.1007/s00359-018-1275-z 1

[8] W. O. Bennett, R. S. Simons, and E. L. Brainerd, "Twisting and Bending: The Functional Role of Salamander Lateral Hypaxial Musculature During Locomotion," *Journal of Experimental Biology*, vol. 204, no. 11, pp. 1979–1989, Jun. 2001. [Online]. Available: https://doi.org/10.1242/jeb.204.11.1979 1

[9] L. J. Shapiro, B. Demes, and J. Cooper, "Lateral bending of the lumbar spine during quadrupedalism in strepsirhines," *Journal of Human Evolution*, vol. 40, no. 3, pp. 231–259, Mar. 2001. [Online]. Available: https://linkinghub.elsevier.com/retrieve/pii/S0047248400904548 1

[10] R. M. Alexander, N. J. Dimery, and R. F. Ker, "Elastic structures in the back and their role in galloping in some mammals," *Journal of Zoology*, vol. 207, no. 4, pp. 467–482, 1985, _eprint: https://onlinelibrary.wiley.com/doi/pdf/10.1111/j.1469-7998.1985.tb04944.x. [Online]. Available: https://onlinelibrary.wiley.com/doi/abs/10.1111/j.1469-7998.1985.tb04944.x 1

[11] N. Schilling and R. Hackert, "Sagittal spine movements of small therian mammals during asymmetrical gaits," *Journal of Experimental Biology*, vol. 209, no. 19, pp. 3925–3939, Oct. 2006. [Online]. Available: https://doi.org/10.1242/jeb.02400 1

[12] W. Haomachai, D. Shao, W. Wang, A. Ji, Z. Dai, and P. Manoonpong, "Lateral Undulation of the Bendable Body of a Gecko-Inspired Robot for Energy-Efficient Inclined Surface Climbing," *IEEE Robotics and Automation Letters*, vol. 6, no. 4, pp. 7917–7924, Oct. 2021, conference Name: IEEE Robotics and Automation Letters. 1

[13] B. Chong, Y. Ozkan Aydin, C. Gong, G. Sartoretti, Y. Wu, J. Rieser, H. Xing, J. Rankin, K. Michel, A. Nicieza, J. Hutchinson, D. Goldman, and H. Choset, "Coordination of back bending and leg movements for quadrupedal locomotion," in *Robotics: Science and Systems XIV*. Robotics: Science and Systems Foundation, Jun. 2018. [Online]. Available: http://www.roboticsproceedings.org/rss14/p20.pdf 1

[14] N. Schilling and D. R. Carrier, "Function of the epaxial muscles in walking, trotting and galloping dogs: implications for the evolution of epaxial muscle function in tetrapods," *Journal of Experimental Biology*, vol. 213, no. 9, pp. 1490–1502, May 2010. [Online]. Available: https://doi.org/10.1242/jeb.039487 1

[15] Q. Zhao, H. Sumioka, K. Nakajima, X. Yu, and R. Pfeifer, "Spine as an engine: effect of spine morphology on spine-driven quadruped locomotion," *Advanced Robotics*, vol. 28, no. 6, pp. 367–378, Mar. 2014, publisher: Taylor & Francis _eprint: https://doi.org/10.1080/01691864.2013.867287. [Online]. Available: https://doi.org/10.1080/01691864.2013.867287 1

[16] R. Ritter, "Lateral bending during lizard locomotion," *Journal of Experimental Biology*, vol. 173, no. 1, pp. 1–10, Dec. 1992. [Online]. Available: https://doi.org/10.1242/jeb.173.1.1 1

[17] P. P. Gambaryan, "How mammals run," *Anatomical Adaptations*, 1974. 2

[18] R. M. Alexander, *Principles of animal locomotion*. Princeton University Press, 2003. 2

[19] P. Eckert, A. E. Schmerbauch, T. Horvat, K. Söhnel, M. S. Fischer, H. Witte, and A. J. Ijspeert, "Towards rich motion skills with the lightweight quadruped robot serval-a design, control and experimental study," in *International Conference on Simulation of Adaptive Behavior*. Springer, 2018, pp. 41–55. 2

[20] M. Khoramshahi, A. Spröwitz, A. Tuleu, M. N. Ahmadabadi, and A. J. Ijspeert, "Benefits of an active spine supported bounding locomotion with a small compliant quadruped robot," in *2013 IEEE international conference on robotics and automation*. IEEE, 2013, pp. 3329–3334. 2

[21] J. Duperret and D. E. Koditschek, "Empirical validation of a spined sagittal-plane quadrupedal model," in *2017 IEEE International Conference on Robotics and Automation (ICRA)*. IEEE, 2017, pp. 1058–1064. 2

[22] D. Chen, N. Li, H. Wang, and L. Chen, "Effect of flexible spine motion on energy efficiency in quadruped running," *Journal of Bionic Engineering*, vol. 14, no. 4, pp. 716–725, 2017. 2

[23] D. Kuehn, A. Dettmann, and F. Kirchner, "Analysis of using an active artificial spine in a quadruped robot," in *2018 4th International Conference on Control, Automation and Robotics (ICCAR)*. IEEE, 2018, pp. 37–42. 2

[24] A. P. Sabelhaus, L. J. van Vuuren, A. Joshi, E. Zhu, H. J. Garnier, K. A. Sover, J. Navarro, A. K. Agogino, and A. M. Agogino, "Design, simulation, and testing of a flexible actuated spine for quadruped robots," *arXiv preprint arXiv:1804.06527*, 2018. 2

[25] M. H. H. Kani, M. Derafshian, H. J. Bidgoly, and M. N. Ahmadabadi, "Effect of flexible spine on stability of a passive quadruped robot: Experimental results," in *2011 IEEE International Conference on Robotics and Biomimetics*. IEEE, 2011, pp. 2793–2798. 2

[26] T. Takuma, M. Ikeda, and T. Masuda, "Facilitating multi-modal locomotion in a quadruped robot utilizing passive oscillation of the spine structure," in *2010 IEEE/RSJ International Conference on Intelligent Robots and Systems*. IEEE, 2010, pp. 4940–4945. 2

[27] J. D. Caporale, B. W. McInroe, C. Ning, T. Libby, R. J. Full, and D. E. Koditschek, "Coronal Plane Spine Twisting Composes Shape To Adjust the Energy Landscape for Grounded Reorientation," in *2020 IEEE International Conference on Robotics and Automation (ICRA)*, May 2020, pp. 8052–8058, iSSN: 2577-087X. 2

[28] G. A. Folkertsma, S. Kim, and S. Stramigioli, "Parallel stiffness in a bounding quadruped with flexible spine," in *2012 IEEE/RSJ International Conference on Intelligent Robots and Systems*. IEEE, 2012, pp. 2210–2215. 2

[29] U. Culha and U. Saranli, "Quadrupedal bounding with an actuated spinal joint," in *2011 IEEE International Conference on Robotics and Automation*. IEEE, 2011, pp. 1392–1397. 2

[30] L. T. Phan, Y. H. Lee, Y. H. Lee, H. Lee, H. Kang, and H. R. Choi, "Study on effects of spinal joint for running quadruped robots," *Intelligent Service Robotics*, vol. 13, no. 1, pp. 29–46, 2020. 2

[31] ——, "Study on quadruped bounding with a passive compliant spine," in *2017 IEEE/RSJ International Conference on Intelligent Robots and Systems (IROS)*. IEEE, 2017, pp. 2409–2414. 2

[32] Y. Yesilevskiy, W. Yang, and C. D. Remy, "Spine morphology and energetics: how principles from nature apply to robotics," *Bioinspiration & biomimetics*, vol. 13, no. 3, p. 036002, 2018. 2

[33] S. Bhattacharya, A. Singla, D. Dholakiya, S. Bhatnagar, B. Amrutur, A. Ghosal, S. Kolathaya *et al.*, "Learning active spine behaviors for dynamic and efficient locomotion in quadruped robots," in *2019 28th IEEE International Conference on Robot and Human Interactive Communication (RO-MAN)*. IEEE, 2019, pp. 1–6. 2

[34] L. Raw, C. Fisher, and A. Patel, "Effects of limb morphology on transient locomotion in quadruped robots," in *2019 IEEE/RSJ International Conference on Intelligent Robots and Systems (IROS)*. IEEE, 2019, pp. 3349–3356. 2

[35] M. Khoramshahi, H. J. Bidgoly, S. Shafiee, A. Asaei, A. J. Ijspeert, and M. N. Ahmadabadi, "Piecewise linear spine for speed–energy efficiency trade-off in quadruped robots," *Robotics and Autonomous Systems*, vol. 61, no. 12, pp. 1350–1359, 2013. 2

[36] C. Fisher, S. Shield, and A. Patel, "The effect of spine morphology on rapid acceleration in quadruped robots," in *2017 IEEE/RSJ International Conference on Intelligent Robots and Systems (IROS)*. IEEE, 2017, pp. 2121–2127. 2

[37] C. Fisher and A. Patel, "On the optimal spine morphology of rapidly accelerating quadrupeds," *SAIEE Africa Research Journal*, vol. 112, no. 3, pp. 126–133, 2021. 2

[38] K. Ye and K. Karydis, "Modeling and trajectory optimization for standing long jumping of a quadruped with a preloaded elastic prismatic spine," in *2021 IEEE/RSJ International Conference on Intelligent Robots and Systems (IROS)*. IEEE, 2021, pp. 902–908. 2

[39] C. D. Remy, K. Buffinton, and R. Siegwart, "Comparison of cost functions for electrically driven running robots," in *2012 IEEE International Conference on Robotics and Automation*, May 2012, pp. 2343–2350, iSSN: 1050-4729. 2, 3

[40] M. Posa, S. Kuindersma, and R. Tedrake, "Optimization and stabilization of trajectories for constrained dynamical systems," in *2016 IEEE International Conference on Robotics and Automation (ICRA)*. Stockholm, Sweden: IEEE, May 2016, pp. 1366–1373. [Online]. Available: http://ieeexplore.ieee.org/document/7487270/ 2

[41] R. Tedrake and the Drake Development Team, "Drake: Model-based design and verification for robotics," 2019. [Online]. Available: https://drake.mit.edu 2

[42] M. Kelly, "An introduction to trajectory optimization: How to do your own direct collocation," *SIAM Review*, vol. 59, no. 4, pp. 849–904, 2017. [Online]. Available: https://doi.org/10.1137/16M1062569 2

[43] J. T. Betts, *Practical Methods for Optimal Control and Estimation Using Nonlinear Programming, Second Edition*, 2nd ed. Society for Industrial and Applied Mathematics, 2010. [Online]. Available: https://epubs.siam.org/doi/abs/10.1137/1.9780898718577 2

[44] M. Posa and DAIRLab, "Dairlib," github.com/DAIRLab/dairlib, 2019. 2

[45] Z. Manchester, N. Doshi, R. J. Wood, and S. Kuindersma, "Contact-implicit trajectory optimization using variational integrators," *The International Journal of Robotics Research*, vol. 38, no. 12-13, pp. 1463–1476, 2019. [Online]. Available: https://doi.org/10.1177/0278364919849235 2

[46] A. M. Johnson and D. E. Koditschek, "Legged self-manipulation," *IEEE Access*, vol. 1, pp. 310–334, 2013. 2

[47] G. Kenneally, A. De, and D. E. Koditschek, "Design principles for a family of direct-drive legged robots," *IEEE Robotics and Automation Letters*, vol. 1, no. 2, pp. 900–907, 2016. 3

[48] Z. Feng, J. D. Caporale, and S. Rozen-Levy, "Quadrupedal morphology study," https://github.com/KodlabPenn/quad-morphology-study, 2022. 3

[49] M. Hildebrand, "Analysis of asymmetrical gaits," *Journal of Mammalogy*, vol. 58, no. 2, pp. 131–156, 1977. 3

[50] M. Haberland and S. Kim, "On extracting design principles from biology: I. method–general answers to high-level design questions for bioinspired robots," *Bioinspiration & biomimetics*, vol. 10, no. 1, p. 016010, 2015.

[51] ——, "On extracting design principles from biology: Ii. case study—the effect of knee direction on bipedal robot running efficiency," *Bioinspiration & biomimetics*, vol. 10, no. 1, p. 016011, 2015.

[52] M. H. H. Kani and M. N. Ahmadabadi, "Comparing effects of rigid, flexible, and actuated series-elastic spines on bounding gait of quadruped robots," in *2013 First RSI/ISM International Conference on Robotics and Mechatronics (ICRoM)*. IEEE, 2013, pp. 282–287.

[53] P. Eckert, A. Spröwitz, H. Witte, and A. J. Ijspeert, "Comparing the effect of different spine and leg designs for a small bounding quadruped robot," in *2015 IEEE International Conference on Robotics and Automation (ICRA)*. IEEE, 2015, pp. 3128–3133.

[54] J. Chen, Z. Liang, Y. Zhu, and J. Zhao, "Improving kinematic flexibility and walking performance of a six-legged robot by rationally designing leg morphology," *Journal of Bionic Engineering*, vol. 16, no. 4, pp. 608–620, 2019.

[55] G. A. Folkertsma, A. J. van der Schaft, and S. Stramigioli, "Morphological computation in a fast-running quadruped with elastic spine," *IFAC-PapersOnLine*, vol. 48, no. 13, pp. 170–175, 2015.